Influence of Mechanical and Electromagnetic Phenomena on Electric Motor Vibrations in Different Power Supply Options

Mateusz WRÓBEL
Poznan University of Technology, Faculty of Mechanical Engineering, 3 Piotrowo St, 60-965 Poznan, mateusz.wrobel@put.poznan.pl

Roman BARCZEWSKI
Poznan University of Technology, Faculty of Mechanical Engineering, 3 Piotrowo St, 60-965 Poznan, roman.barczewski@put.poznan.pl

Bartosz JAKUBEK
Poznan University of Technology, Faculty of Mechanical Engineering, 3 Piotrowo St, 60-965 Poznan, bartosz.jakubek@put.poznan.pl

Wojciech RUKAT
Poznan University of Technology, Faculty of Mechanical Engineering, 3 Piotrowo St, 60-965 Poznan, wojciech.rukat@put.poznan.pl

Abstract

Results of research about influence of mechanical and electromagnetic phenomena on electric motor vibration in different supply options has been shown in this paper. Three different supply options have been taken under consideration: typical star connection, single-phase connection with work capacitor and connection through an inverter. Vibration signals recorded on electric motor end shield and frame has been digitally processed using Multi-Synchronous Averaging (MSA). This technique allowed to decompose total vibration signal into signals associated with mechanical and electromagnetic phenomena occurring in electric motor. The comparison of rms values and spectra shapes of total and decomposed vibration signals has been made. Energy shares of previously mentioned phenomena in vibration signal for different supply options has been also estimated.

***Keywords*:** electric motor, vibration, supply, star, single-phase, inverter, multi-synchronous averaging

1. Introduction

Asynchronous electric motors (AEM) are used as drive units in over 90% of machinery and devices [1, 2]. The common use of this type of motors is due to their reliability, simplicity of construction and a small number of elements susceptible to mechanical damage (mainly rotor and roller bearings), as well as a relatively low price. As a result of the widespread use of electric motors, it is important to keep them in good technical condition and to reduce the number of defective units released on the market. In practice, various techniques and methods are used to test electric motors, such as specialist electrical measurements, e.g. MCSA method (Motor Current Signature Analysis) [3, 4], specialized electric analyses and measurements [4-6], measurements and analyses of vibrations [7, 8] and noise [9, 10], measurements and analyses of magnetic field [11, 12], thermal measurements [13, 14] and others [15].

Defects and damage of asynchronous electric motors can affect both mechanical and electrical parts. Rolling bearing damage, rotor unbalance, misalignment and bending of the motor shaft can occur in the mechanical part. Furthermore, the damage and defects of the electrical part may include: inter-winding short circuits, interruption of stator windings, connection errors and occurrence of undesirable electromagnetic phenomena [16, 17]. Each of the above-mentioned defects and damage affect motor vibrations to varying degrees. Usually the intensity of vibrations recorded on the frame or end shields may indicate the degree of damage and the general technical condition of the motor. Therefore, the vibration signal can be used as a source of information on the technical condition of the electric motor for post-production testing and operational diagnostics.

On the other hand, vibrations resulting from electromagnetic phenomena occurring in electric motors can be largely related to the way the motor is connected to the power supply. In diagnostic applications which use vibrations recorded on the motor frame to assess the technical condition of electric motors it is important to determine the signal components associated with defects or damage to individual motor elements which are movable mechanical parts (e.g. bearings, rotor) and those related to electrical phenomena as well as the way of operation and construction of electromagnetic circuits (slot frequency, magnetostriction phenomenon).

The aim of the research presented in this article was to show qualitative (spectral composition) and quantitative (rms values of motor frame and end shield vibration acceleration) differences resulting from the change in the way the engine is powered. The knowledge of these conditions can be a starting point for the development of diagnostic methods basing on the measurement and analysis of vibroacoustic signals used in both post-production and operational diagnostics. The tests were carried out for the following types of three-phase asynchronous electric motor connections:

- direct star connection to a three-phase power supply; this type of connection is used in the case of continuous operation without the possibility of speed control, however, it is characterized by high starting current,
- connecting a three-phase motor as a single-phase motor using a run capacitor; it enables continuous operation without the possibility of speed control; this solution does not allow to achieve the rated engine power, there is also an undesirable effect in the form of increased engine temperature,
- connection to a three-phase network via an inverter; it makes possible to control the engine rotation speed.

Application of Multi-Synchronous Averaging (MSA) technique allowed to separate the vibration signal into signals related to mechanical and electromagnetic phenomena [18, 19]. The results of decomposition were the basis for estimating the energy share of these phenomena for different options of motor power supply. It also shows to what extent this share depends on the location of vibration transducers (frame, end shield).

2. Tested electric motor and its power supply options

The object of the research was a three-phase asynchronous electric motor type Sh71-4A. The view of the motor with vibration acceleration sensors and an eddy current sensor (tachometer probe) is shown in Fig. 1. The motor is mounted on a concrete block with a mass of 12 kg. Between the motor feet and the block and between the block and the ground there were rubber spacers. Their task was to separate vibrations from the ground. The basic technical parameters of the tested motor are shown in Tab. 1.

Table 1. Basic technical parameters of the tested asynchronous electric motor type Sh71-4A

Rated power	0.25 kW
Supply voltage (Δ / Y)	230 / 400 V
Rotation speed	1380 rpm
Efficiency	66 %

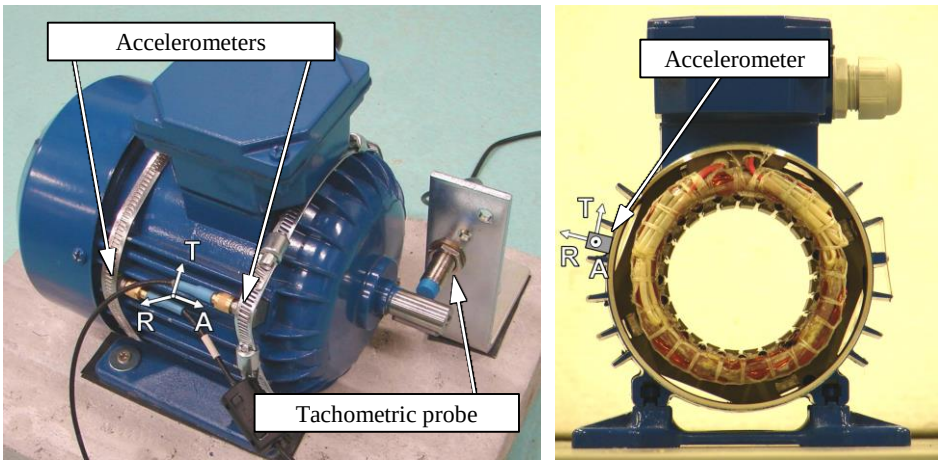


Figure 1. Arrangement of accelerometers and marking of measuring directions as well as a view of the motor frame after dismounting of end shields and the rotor with marked place of mounting of the accelerometer

Fig. 2 shows three alternative ways to connect the motor to the power supply: a typical three-phase star connection, a connection via an inverter and a connection as a single-phase motor with a run capacitor.

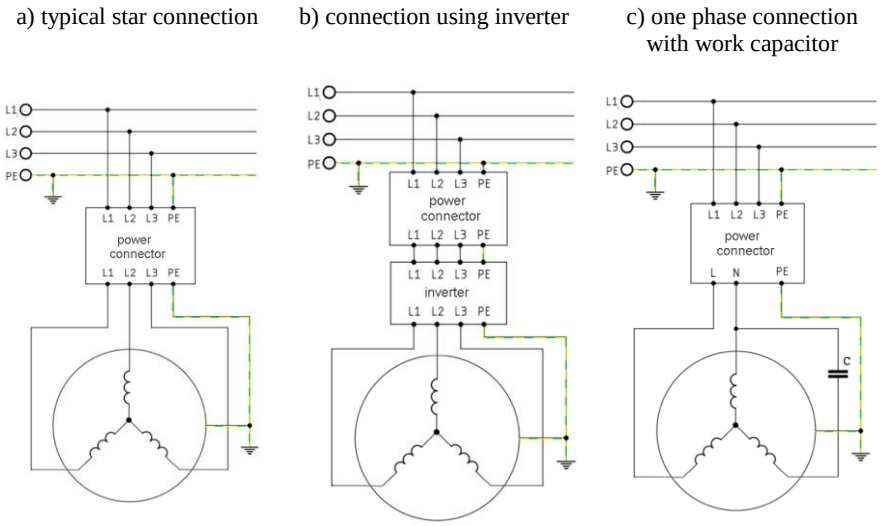


Figure 2. Power supply options of the tested AEM

3. Research methodology

During the tests, synchronous recording of vibrations of the motor frame and the end shield was carried out for each of the previously mentioned types of connections. Vibration accelerations were recorded using two DYTRAN 3023M2 triaxial accelerometers. One of the sensors was mounted on the front end shield and the other on the motor frame. The experiment conducted in this way made it possible to determine the impact of changing the power supply option on vibrations in these locations and in individual directions. Fig. 1b shows the places where the stator has no contact with the motor frame. An accelerometer was mounted at one of these points.

Three directions of vibration recording were adopted: radial R (normal to the frame), tangential to the frame T and axial A (Fig. 1a). The measurement chain was supplemented with dedicated electronic devices for measuring the rotational frequency of the rotor and for tracking the frequency of the 230V power supply. These signals were used as synchronizing signals in the process of multi-synchronous decomposition. The vibration acceleration signal and the tachometer and supply frequency signals were recorded synchronously using TEAC LX-10 8-channel data recording system. The application for recording and analysis of vibration signals was developed in the DASYLab[1] environment. A diagram of the measurement chain is shown in Fig. 3.

[1] DASYLab – Data Acquisition System Laboratory

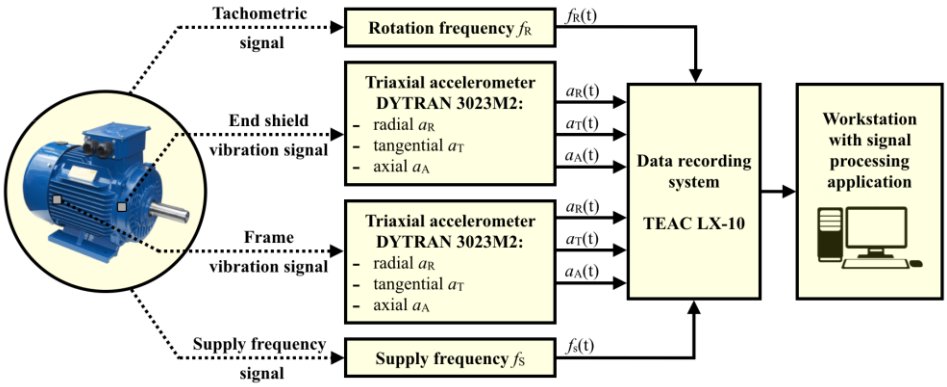


Figure 3. Diagram of the measurement chain

The vibration signal coming from an accelerometer mounted on the motor frame or end shield can be treated as a superposition of signals related to phenomena of mechanical nature (synchronous with rotor frequency f_r), electromagnetic nature (synchronous with mains frequency f_s), as well as components non-synchronous with f_s and f_r and noise. The form of acceleration of such a signal can therefore be written as:

$$a(t) = a^{M}(t) + a^{E}(t) + a^{N}(t), \tag{1}$$

where:

$a(t)$ – recorded vibration acceleration signal,
$a^{M}(t)$ – signal components related to mechanical phenomena (synchronous with f_r),
$a^{E}(t)$ – signal components related to electromagnetic phenomena (synchronous with f_s),
$a^{N}(t)$ – signal components non-synchronous with f_s and f_r and noise.

In the discretization process (ADC), the signal described by formula 1 takes the form of a time series:

$$a_i = a_i^{M} + a_i^{E} + a_i^{N}, \tag{2}$$

where:

i – consecutive number of a signal sample.

Multi-synchronous averaging (MSA) was used for decomposition of vibration signals [18, 19]. The simplified idea of MSA is shown in Fig. 4.

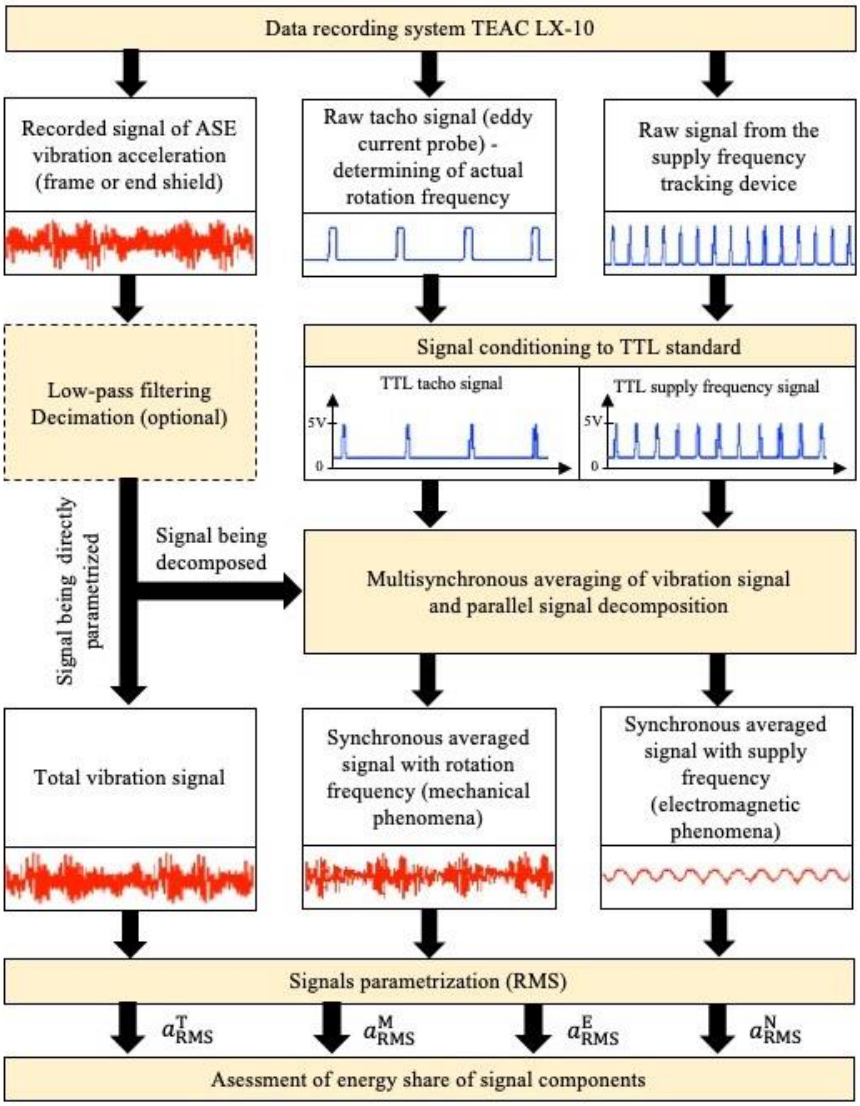


Figure 4. Simplified idea of decomposition of vibration acceleration signals of an asynchronous electric motor by the multi-synchronous averaging technique (MSA)

MSA enables multi-threaded signal decomposition and obtaining mono-periodic polyharmonic signals a_i^{M} and a_i^{E}. An example of functioning of the MSA procedure and reduction of non-synchronous components with f_s and f_r is shown in Fig. 5, which illustrates changes in spectral composition observed in subsequent iterations of synchronous averaging of signals.

a) synchronization with rotation frequency (f_r) b) synchronization with supply frequency (f_s)

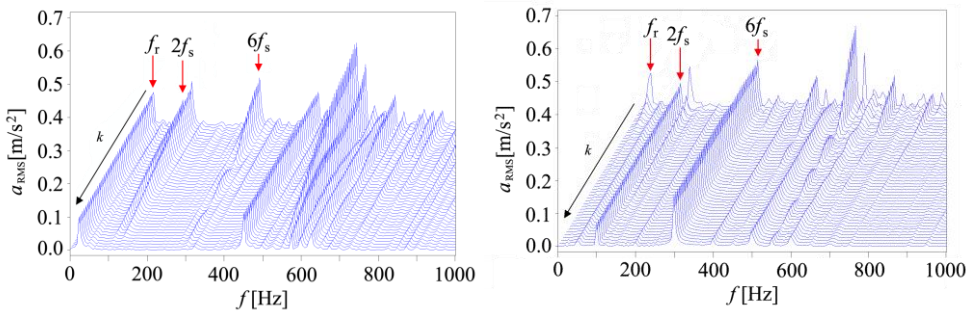


Figure 5. Changes in the spectral composition of vibration acceleration signals averaged synchronously; process synchronized with the supply frequency f_s and rotational frequency of the rotor f_r (k - subsequent iterations of synchronous averaging)

The effective reduction of the $2f_s$ and $6f_s$ frequency components (non-synchronous with f_r) is clearly visible in Fig. 5a, while the reduction of the f_r frequency component is observed in Fig. 5b for averaging synchronization with the f_s frequency. To synchronize the decomposition process, the tachometric signal (associated with f_r) and the supply frequency signal (f_s) were used respectively. In the process of synchronous averaging we obtain signal components $\bar{a}_j^{\mathrm{M}}$ and $\bar{a}_j^{\mathrm{E}}$ representing signals a_i^{M} and a_i^{E} in the form of a time series with a finite number of samples j = 0, 1, ..., N - 1. The correctness of such mapping increases with the number of k (k = 1, 2, ..., K) averaged sequences in the MSA process. The number of averaged K sequences can be determined arbitrarily assuming the desired reduction of non-synchronous components and noise in the averaged signal according to the relationship [20]:

$$K > \left(\frac{1}{R}\right)^2 \tag{3}$$

where:

R – assumed reduction of noise and non-synchronous components (e.g. R = 0.01).

Synchronously averaged signals associated with f_r and f_s can be written as:

$$\bar{a}_j^{\mathrm{M}} = \frac{1}{K}\sum_{k=1}^{K} a_{k,j}^{\mathrm{M}} \;;\; \bar{a}_j^{\mathrm{E}} = \frac{1}{K}\sum_{k=1}^{K} a_{k,j}^{\mathrm{E}}\,, \tag{4}$$

where:

k – consecutive number of sequence of the signal to be averaged (k = 1, 2, …, K),

j – signal sample number in sequences (j = 0, 1, …, N – 1),

N – number of signal samples in the sequences of the signals to be averaged.

In the next processing step, the rms values of the signal subjected to decomposition a_i and signals $\bar{a}_j^{\mathrm{M}}$ and $\bar{a}_j^{\mathrm{E}}$ synchronously averaged are determined:

$$a_{\mathrm{RMS}}^{\mathrm{T}} = \sqrt{\frac{1}{L}\sum_{i=0}^{L-1} a_i^2} \; ; \; a_{\mathrm{RMS}}^{\mathrm{M}} = \sqrt{\frac{1}{N}\sum_{j=0}^{N-1} (\bar{a}_j^{\mathrm{M}})^2} \; ; \; a_{\mathrm{RMS}}^{\mathrm{E}} = \sqrt{\frac{1}{N}\sum_{j=0}^{N-1} (\bar{a}_j^{\mathrm{E}})^2} \; , \tag{5}$$

where:

L – number of samples of the total signal to be decomposed (it is justified that $L \geq N \cdot K$).

Bearing in mind the signal form described by formulas 1 or 2, the following relationship can be formulated in terms of signal power:

$$\mathrm{P}^{\mathrm{T}} = \mathrm{P}^{\mathrm{M}} + \mathrm{P}^{\mathrm{E}} + \mathrm{P}^{\mathrm{N}}, \tag{6}$$

where:

P^{T} – power of total signal a_i,

P^{M}, P^{E}, P^{N} – powers of signal components associated with mechanical (M), electromagnetic phenomena, respectively (E) and other components (N) - non-synchronous with f_s and f_r, and noise.

It can be assumed that relation 6 for $K \to \infty$ in terms of rms values will take form:

$$(a_{\mathrm{RMS}}^{\mathrm{T}})^2 = (a_{\mathrm{RMS}}^{\mathrm{M}})^2 + (a_{\mathrm{RMS}}^{\mathrm{E}})^2 + (a_{\mathrm{RMS}}^{\mathrm{N}})^2. \tag{7}$$

On this basis, for a finite number of averagings $k = K$, the rms value of non-synchronous signals and noise can be estimated according to the relation:

$$a_{\mathrm{RMS}}^{\mathrm{N}} \cong \sqrt{(a_{\mathrm{RMS}}^{\mathrm{T}})^2 - (a_{\mathrm{RMS}}^{\mathrm{M}})^2 - (a_{\mathrm{RMS}}^{\mathrm{E}})^2}. \tag{8}$$

With the rms values and powers of the total and decomposed vibration acceleration signals, a multivariant analysis of the influence of asynchronous power supply method of an electric motor on the vibrations of its frame and end shield was performed.

4. Results

Based on the summary of the rms values of the total vibration acceleration signal (Tab. 2 and Fig. 6), recorded both on the front end shield of the motor and on its frame, it can be stated that:

- the typical star connection allows the smallest motor vibroactivity to be achieved; the vibration acceleration values in the 10-10000 Hz band for individual directions are close to 0.5 m/s^2; the dominant amplitude components of the signals are in the band up to approx. 1000 Hz (Fig. 5);
- the single-phase connection with a run capacitor results in approx. 2.5-fold increase in the rms values of the vibration accelerations (vector sum), both on the end shield and the motor frame, with the greatest changes in the axial direction;

- the use of an inverter has resulted in an approx. 7-fold increase in the rms values of vibration acceleration compared to the star connection; this is mainly due to the appearance of additional amplitude dominant components in the 4-6 kHz and 9-11 kHz bands (Fig. 7) related to the specific operation of the applied inverter, and more precisely to the frequency of the generated PWM signal [21, 22]; in the above-mentioned bands a 5 kHz pulse frequency and modulation side bands are included.

Table 2. Results summary of rms values of vibration signal after multi-synchronous decomposition measured on end shield and motor frame in different supply options

STAR CONNECTION	vibration acceleration a_{RMS} [m/s^2]							
	end shield				frame			
	axial	tang.	radial	vect. sum	axial	tang.	radial	vect. sum
total	**0.53**	**0.58**	**0.56**	**0.97**	**0.59**	**0.59**	**0.36**	**0.91**
mechanical phenomena	0.23	0.26	0.26	0.44	0.25	0.28	0.17	0.41
electromagnetic phenomena	0.17	0.30	0.19	0.40	0.20	0.32	0.12	0.39
residual	0.44	0.42	0.47	0.77	0.49	0.41	0.30	0.71
SINGLE-PHASE CONNECTION	end shield				frame			
	axial	tang.	radial	vect. sum	axial	tang.	radial	vect. sum
total	**1.69**	**1.18**	**0.98**	**2.28**	**1.86**	**1.18**	**0.93**	**2.39**
mechanical phenomena	0.60	0.28	0.38	0.76	0.63	0.57	0.39	0.93
electromagnetic phenomena	1.30	0.92	0.54	1.69	1.45	0.67	0.59	1.70
residual	0.90	0.67	0.72	1.33	0.98	0.78	0.61	1.40
INVERTER	end shield				frame			
	axial	tang.	radial	vect. sum	axial	tang.	radial	vect. sum
total	**5.32**	**4.78**	**3.27**	**7.87**	**2.99**	**5.52**	**2.28**	**6.68**
mechanical phenomena	0.62	0.66	0.43	1.00	0.40	0.70	0.31	0.86
electromagnetic phenomena	0.89	1.10	0.63	1.55	0.57	1.01	0.44	1.24
residual	5.21	4.61	3.18	7.65	2.90	5.38	2.22	6.50

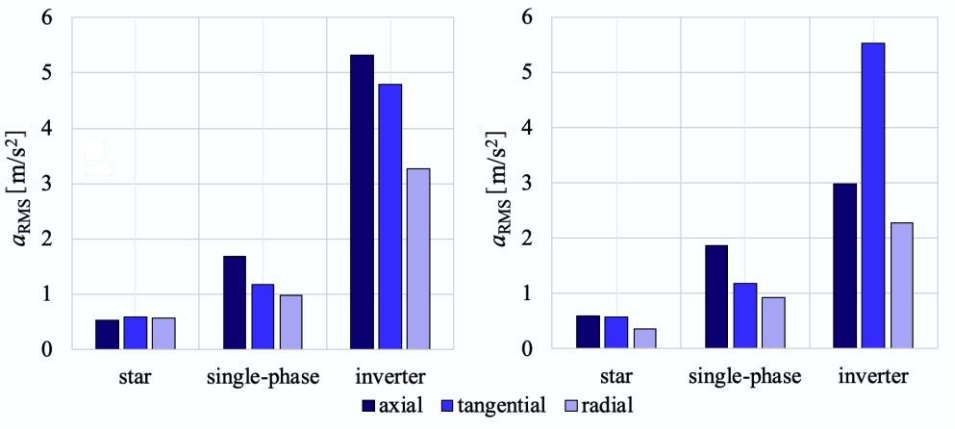


Figure 6. Vibration accelerations of the end shield and motor frame in three directions for different types of connection of motor to the power supply

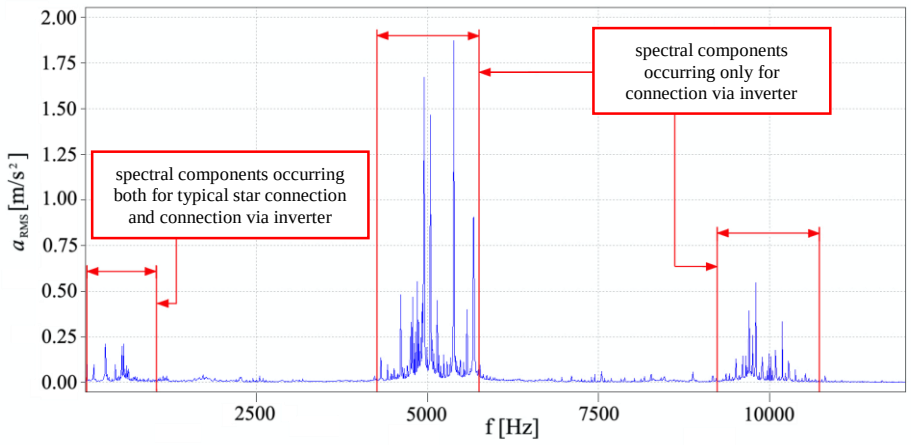


Figure 7. Example of a motor frame vibration acceleration spectrum illustrating the appearance of additional signal components resulting from the use of an inverter

Considering the use of vibrations as a carrier of information in diagnostics (e.g. post-production or operational), it would be justified to base diagnostic inference procedures on rms values obtained as a result of the MSA decomposition. The results of the decomposition are given in the Tab. 2. In addition to the rms values of vibration accelerations of mechanical and electromagnetic phenomena, rms values of components of signals non-synchronous with f_s and f_r and noise (residual components) determined in accordance with formula 8 are also provided.

Based on this data and Fig. 8-9 containing the power shares of individual signal components, the following conclusions can be drawn:

- the largest share of components synchronous with f_s and f_r at the star connection was recorded both on the motor body and on the bearing shield for measurements in the tangential direction (approx. 50%); this means that for this type of connection we obtain the best SNR ratio; also, for this direction the shares of components related to mechanical and electromagnetic phenomena are comparable (in the order of 20% - 30%),
- the single-phase connection causes a significant increase in the share of components associated with electromagnetic phenomena, depending on the direction, up to approx. 60%; this is due to an increase in the $2f_s$ component (100 Hz - magnetostriction),
- the use of the inverter in the motor power supply system results in the appearance of additional high-energy components non-synchronous with f_s and f_r, which is visible in a radical increase in their share in the signal (up to over 90%); this may cause masking of components related to mechanical and electromagnetic phenomena associated with f_s and f_r.

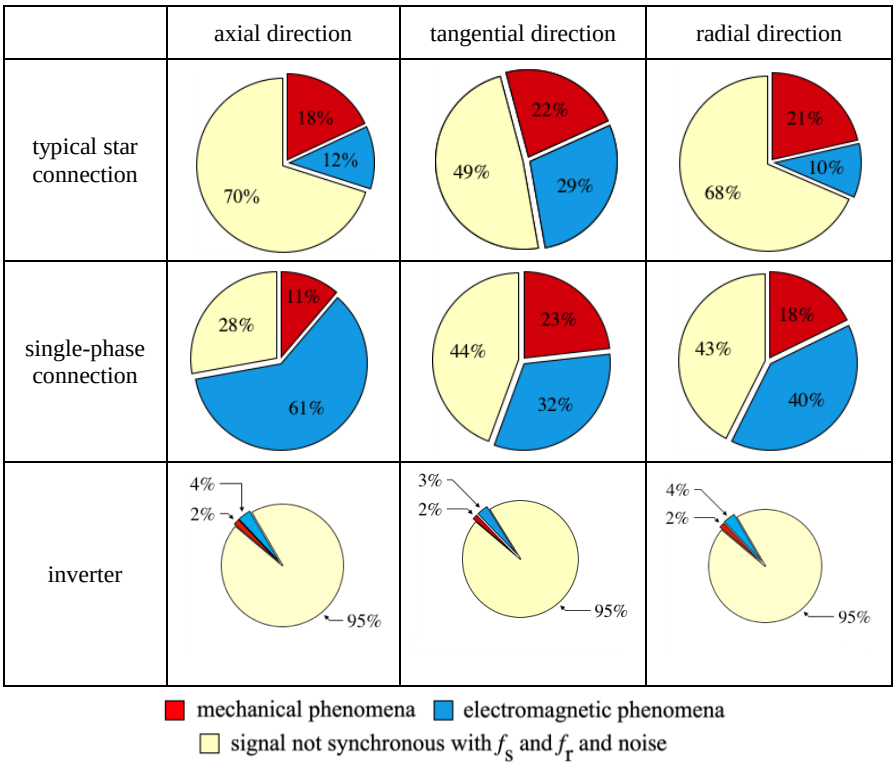


Figure 8. Summary of results of multi-synchronous decomposition of the vibration acceleration signal recorded on the motor frame

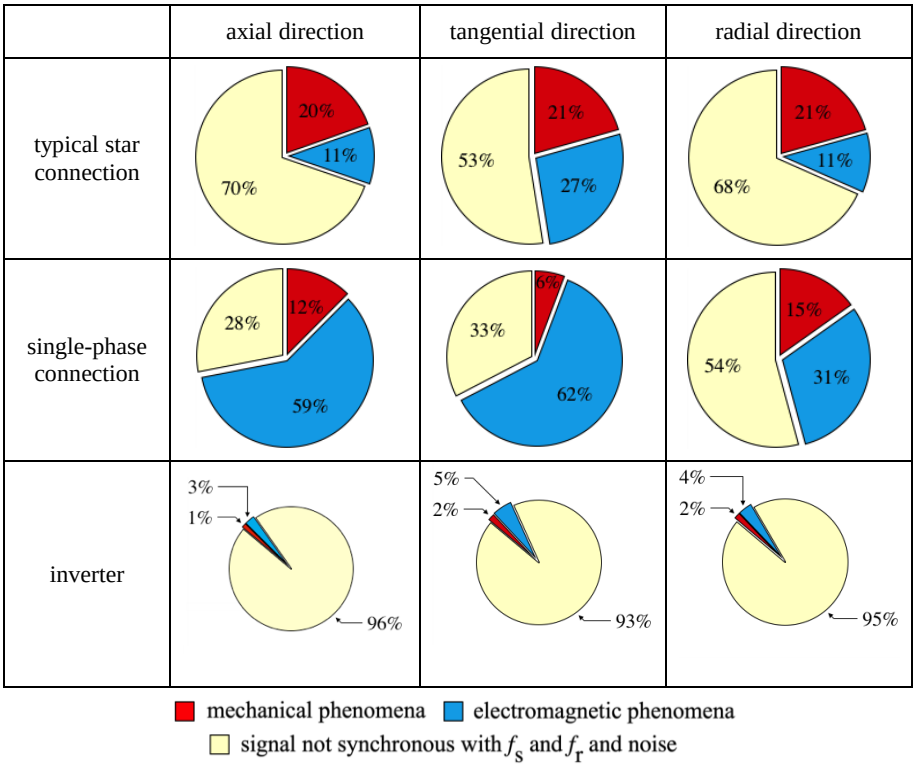


Figure 9. Summary of results of multi-synchronous decomposition of the vibration acceleration signal recorded on the front end shield of the motor

5. Conclusions

The conducted research allowed us to conclude that the application of the process of multi-synchronous decomposition in the diagnostics of asynchronous electric motors gives positive effects. It is possible to extract information on mechanical and electromagnetic phenomena from the vibration signal.

Considering the test results obtained, it is advisable to diagnose motors when they are connected in a star; this is supported by obtaining comparable rms values regardless of the location of the measuring transducer. Connection by an inverter potentially gives information about the motor's susceptibility to vibrations mainly in the band of approx. 5 kHz. This may be particularly important if the motor structure will have its own natural frequencies in this band. This may result in an increased noise level. The 5 kHz frequency band coincides with the most sensitive band of the human hearing organ [22].

Carrying out tests on a larger number of motors of the same type would make it possible to specify these regularities and, in terms of application, would provide the basis for determining the thresholds for classifying the motor quality in terms of electrical

and mechanical performance. In further tests of motors connected to the power supply via an inverter, it is justified to use a third signal synchronizing the multi-synchronous decomposition process related to the pulse frequency of the inverter obtained from the PWM signal. As a result, a three-stream MSA decomposition would be possible.

Acknowledgments

The work was financed by science grant 02/21/SBAD/3558 from the Ministry of Science and Higher Education.

References

1. T. Glinka, *Diagnosing of electrical machinery* (in Polish), in: Inżynieria diagnostyki maszyn, Ed. B. Żółtowski, C. Cempel, PIB, Radom 2004, 633 – 654.
2. F. Ohnacker, *Maintenence of Electrical Equipment*, in: Maintenance Engineering Handbook, Ed. L.R. Higgins, Nowy Jork 1988, 7-1 – 7-28.
3. D. Miljković, *Brief Reviev of Motor Current Signature Analysis*, HDBKR Info Magazin, **5** (2015) 14 – 26.
4. K. Roczek, T. Rogala, *Induction Motor Diagnosis with use of electric parameters*, Diagnostyka, 20 (2019) 65 – 74.
5. S. A. Bednarz, M. Dybkowski, *Induction motor windong faults detection using flux-error based MRAS estimators*, Diagnostyka, **20** (2019) 87 – 96.
6. M. Boudiaf, L. Cherroun et al., *Real-time diangosisof three-phase induction motor machine using Arduino-UNO card based on Park's circle method*, Diagnostyka, **19** (2018) 63 – 71.
7. H. Çalis, *Vibration and motor current analysis of induction motors to diagnose mechanical faults*, Journal of Measurements in Engineering, **2** (2014) 190 – 198.
8. H. Bate, *Vibration Diagnostics for Industrial Electric Motor Drives*, Bruel & Kjaer Application Note, BO-0269-12, 1990.
9. P. A. Delgado-Arredondo, D. Morinigo-Sotelo et al., *Methodology for fault detection in induction motors via sound and vibration signals*, Mechanical Systems and Signal Processing, **83** (2017) 568 – 589.
10. M. Serrazin, S. Gillijns et al., *Vibro-acoustic measurements and techniques for electric automotive applications*, Proceedings of 43rd International Congress on Noise Control Engineering Internoise, 2014, 5128 – 5137.
11. J. Tulicki, J. Petryna et al., *Fault diagnosis of induction motors in selected working conditions based on axial flux signals*, Technical Transactions: Electrical Engineering, **3-E** (2016) 99 – 113.
12. J. Petryna, M. Sułowicz et al., *The use of axial flux in dynamic states testing of low and high power induction machines* (in Polish), Zeszyty Problemowe – Maszyny Elektryczne, **2** (2014) 165 – 171.
13. I. Gavranic, M. Vrazic et al., *Induction motor rotor cage faults as ignition sources of explosive atmosphere – research on heating*, Technicki Vjesnik, **24** (2017) 1025 – 1031.

14. D. Staton, L. Šušnjić, *Induction Motor Thermal Analysis*, Strojarstvo, **51** (2009) 623 – 631.
15. A. Regaz, B. Zegnini, et al., *Detection of faults in the asynchronous machine by the use of smart materials*, Diagnostyka, **19** (2018) 43 – 54.
16. K. K. Pandey, P. H. Zope et al., *Review on Fault Diagnosis in Three-Phase Induction Motor*, MEDHA, **1** (2012), 53 – 58.
17. M. R. Mehrjou, N. Mariun et al., *Rotor fault condition monitoring techniques for squirrel-cage induction machine — A review*, Mechanical Systems and Signal Processing, **25** (2011) 2828 – 2848.
18. M. Lebold, K., McClintic et al., *Review of vibration analysis methods for gearbox diagnostics and prognostics*, Proceedings of the 54th Meeting of the Society for Machinery Failure Prevention Technology, (2000) 623 – 634.
19. I. Bravo-Imaz, H. Ardakani et al., *Motor current signature analysis for gearbox condition monitoring under transient speeds using wavelet analysis and dual-level time synchronous averaging*, Mechanical Systems and Signal Processing, **94** (2017) 73 – 84.
20. S. Brown, *Discover Signal Processing – An Interactive Guide for Engineers*, John Wiley & Sons Ltd, Chichester 2008, 265 – 269.
21. Hitachi Industrial Equipment Systems Co., Ltd., *User manual: SJ200 inverter* (in Polish), **NB650XA** (2004).
22. J. Guziński, Z. Krzemiński, *Output filter of voltage inverter* (in Polish), Napędy i Sterowanie, **4** (2005) 43 – 44.
23. Z. Żyszkowski, *Basics of electroacoustics* (in Polish), Wydawnictwo Naukowo-Techniczne, Warszawa 1984, 228 – 261.